Title

Coronary artery endothelial cells and microparticles increase expression of VCAM-1 in myocardial infarction

Journal

Thrombosis and Haemostasis, 113(03)

ISSN

0340-6245

Authors

Radecke, Christopher E
Warrick, Alexandra E
Singh, Gagan D
et al.

Publication Date

2015-05-01

DOI

10.1160/th14-02-0151

Peer reviewed

Published in final edited form as:

Thromb Haemost. 2015 March ; 113(3): 605–616. doi:10.1160/TH14-02-0151.

Coronary artery endothelial cells and microparticles increase expression of VCAM-1 in myocardial infarction

Christopher E. Radecke[1], **Alexandra E. Warrick**[2], **Gagan D. Singh**[2], **Jason H. Rogers**[2], **Scott I. Simon**[1], and **Ehrin J. Armstrong**[3,4]

[1]Department of Biomedical Engineering, University of California, Davis, Davis, California, USA

[2]Division of Cardiovascular Medicine, University of California, Davis, Medical Center. Sacramento, California, USA

[3]Division of Cardiology, University of Colorado, Denver, Colorado, USA

[4]VA Eastern Colorado Healthcare System, Denver, Colorado, USA

Summary

Coronary artery disease (CAD) is characterised by progressive atherosclerotic plaque leading to flow-limiting stenosis, while myocardial infarction (MI) occurs due to plaque rupture or erosion with abrupt coronary artery occlusion. Multiple inflammatory pathways influence plaque stability, but direct assessment of endothelial inflammation at the site of coronary artery stenosis has largely been limited to pathology samples or animal models of atherosclerosis. We describe a technique for isolating and characterising endothelial cells (ECs) and EC microparticles (EMPs) derived directly from the site of coronary artery plaque during balloon angioplasty and percutaneous coronary intervention. Coronary artery endothelial cells (CAECs) were identified using imaging flow cytometry (IFC), and individual CAEC and EMP expression of the pro-atherogenic adhesion molecule vascular cell adhesion molecule-1 (VCAM-1) was assessed immediately following angioplasty. Patients with MI registered 73 % higher VCAM-1 expression on their CAECs and 79 % higher expression on EMPs compared to patients with stable CAD. In contrast, VCAM-1 expression was absent on ECs in the peripheral circulation from these same subjects. VCAM-1 density was significantly higher on CAECs and EMPs among patients with MI and positively correlated with markers of myocardial infarct size. We conclude that increased VCAM-1 expression on EC and formation of EMP at the site of coronary plaque is positively correlated with the extent of vascular inflammation in patients with myocardial infarction.

Keywords

Acute myocardial infarction; adhesion molecules; VCAM-1; endothelial cells; inflammation; microparticles

Correspondence to: Scott I. Simon, Department of Biomedical Engineering, University of California at Davis, 451 East Health Sciences Drive, Davis, CA 95616, USA, Tel.: +1 530 752 0299, sisimon@ucdavis.edu.

Conflicts of interest

None declared.

Introduction

Cardiovascular disease remains the most common cause of death in the U. S. (1, 2). Coronary artery disease (CAD) is characterised by symptoms of stable angina, while myocardial infarction (MI) occurs as a result of plaque rupture or erosion, typically without antecedent symptoms. Following an MI, up to 20 % of patients subsequently develop recurrent MI or heart failure (3, 4). Although increased inflammation portends a higher risk of subsequent events, there are few *in vivo* measures of emerging biomarkers collected at the site of the coronary artery plaque. Functional analysis of plaque-derived coronary artery endothelial cells (CAECs) and endothelial microparticles (EMPs) could identify novel interventions to reduce the risk of subsequent events and also improve risk stratification for secondary prevention of CAD.

Endothelial cell (EC) vascular cell adhesion molecule-1 (VCAM-1) is a pro-atherogenic adhesion molecule central to both initiation of atherosclerosis and progression towards plaque instability (5–9). Both circulating VCAM-1 levels and EMP number have been associated with increased risk of adverse outcomes after MI (10, 11), but no studies have reported the levels of plaque endothelial VCAM-1 expression or the relationship of EC activation to EMP formation. Local shear stress conditions (e. g. disturbed flow, low time-varying shear stress), and epigenetic changes (e. g. elaboration of endothelial superoxide dismutase and nitric oxide synthase) likely account for significant EC heterogeneity within the coronary arteries relative to other vascular beds (12, 13). Moreover, ECs at the site of plaque formation are exposed to microenvironments that can lead to increased adhesion receptor and cytokine expression, EMP formation, and increased apoptosis (5, 14–17).

Previous approaches to collecting ECs during peripheral or coronary angiography retrieved cells adherent to guidewires (18, 19). However, these methods have been limited by low cell yield and absence of a means to reliably compare cell number and activation state between individuals. To address these limitations, we developed a technique to identify and enumerate ECs from coronary artery blood collected during balloon angioplasty. Flow cytometry was used to quantify CAEC and EMP number and expression of VCAM-1 from coronary samples collected from patients with stable CAD or MI, and imaging flow cytometry (IFC) facilitated morphologic analysis of EC and EMP phenotype and VCAM-1 receptor density. These results demonstrate the utility of CAECs and EMPs as markers of local plaque instability and as potential mediators of the inflammatory injury that occurs during MI.

Materials and methods

Patients and blood isolation

Blood samples were collected from 72 subjects undergoing percutaneous coronary interventions (PCI) for treatment of symptomatic stable CAD (n=47) or MI (n=25). All patients provided informed consent from an institutional approved IRB of the University of California, Davis. Patients with stable CAD were diagnosed based on presentation with exertional substernal chest pressure without recent acceleration in symptoms and evidence of a significant angiographic stenosis ≥ 70 %, in the absence of myocardial necrosis.

Patients with MI were diagnosed by a presentation of chest pressure, electrocardiographic changes, elevated troponin consistent with MI, and angiographic evidence of a flow-limiting coronary artery stenosis with associated thrombus. All patients with MI were treated within 12 hours (h) of initial symptom onset. SYN-TA × score and lesion length were classified using quantitative coronary angiography. Myocardial blush was scored after intervention from 0–3 (20). Corrected TIMI frame counts were also scored for each infarct-related artery (21). Patient characteristics are detailed in Table 1.

During PCI, a guide catheter was advanced to the ostium of the coronary artery. A 0.014" guide wire was advanced across the target lesion, while taking care to minimise disruption of the culprit plaque. An angioplasty balloon was then advanced to the site of the plaque and inflated to the size of the reference artery. All of the initial angioplasty balloons were 2.0–3.0 mm in diameter (sized to the reference vessel) and 12–15 mm in length. Immediately after deflation of the balloon, 10 ml of coronary artery blood was aspirated from the guiding catheter, and the balloon was also removed through the catheter and retrieved for further analysis. The sequence of this methodology is depicted in Figure 1. After blood aspiration and balloon retrieval, the remainder of the PCI was carried out as clinically indicated. Blood samples were immediately stored on ice in ethylenediaminetetraacetic acid vacutainers (BD, Franklin Lakes, NJ, USA; 367844), to prevent platelet degranulation. Balloon samples used during procedures were also retrieved and stored in 2 ml of 1 mM ethylenediaminetetraacetic acid dissociation buffer to facilitate collection of any CAECs adherent to the balloon. Processing of the samples was performed within 1 h of blood draw and balloon collection.

Flow cytometry

Flow cytometry provided rapid multiparametric analysis using a five-parameter, three-color FACScan (BD Biosciences, San Jose, CA, USA). Two isolation techniques were employed: a mononuclear cell (MNC) isolation technique was used for analysis of isolated CAECs, while a blood lysis was used to compare the efficiency of CAEC detection and for collection of EMPs. Antibodies were titrated to achieve optimal working concentrations to maximise the specific signal to background fluorescence. AccuCheck cell counting beads (Life Technologies, Carlsbad, CA, USA; PCB100) comprised of two different bead diameters with defined concentrations were used to ensure homogenous sampling during acquisition on the FACScan. Sampling was deemed homogeneous if equal numbers of the two bead populations were acquired (Suppl. Figure 1, available online at www.thrombosis-online.com). Spherotech 6-Peak Rainbow beads (Spherotech, Lake Forest, IL, USA; URCP-38–2K) were used to quality control the FACScan flow cytometer and ensure consistent performance and prevent drift in photomultiplier tube and photodiode voltage.

MNC isolation technique

For CAEC analysis, MNC buffy coat layers were isolated from coronary artery blood samples by Lymphoprep (Accurate Chemicals and Scientific Corporation, Westbury, NY, USA; AN1001967) density centrifugation (d = 1.077 g/ml) and resuspended in FACS buffer (HBSS without Ca^{2+} and Mg^{2+}, supplemented with 0.1 % human serum albumin). 10 ml of coronary artery blood, acquired as described above, were diluted in 15ml FACS buffer (1:

1.5 ratio), layered on top of 12.5 ml Lymphoprep (2: 1 ratio) and centrifuged for 25 minutes (min) at room temperature at 800g. The MNC buffy coat band was isolated, washed in 50 ml of FACS buffer, and pelleted by centrifugation for 10 min at room temperature at 250g. Cells were re-suspended and counted on a haemocytometer. 3×10^6 cells were distributed to each of four polystyrene tubes – a sample to be stained in the presence of all antibodies (all stained sample) and three fluorescence minus one (FMO) gating controls – one for each fluorochrome used within the all stain sample (49–51). Prior to staining, cells were incubated with 140 μg/ml human IgG (R&D Systems, Minneapolis, MN, USA; 1–001-A) on ice for 20 min to block fragment crystalisable (Fc) receptor-mediated binding. Staining was performed with AF488-CD146 (melanoma cell adhesion molecule, MCAM, S-endo-1) (Clone: SHM-57, Biolegend, San Diego, CA, USA; 342008), PE-CD106 (VCAM-1) (Clone: STA, Biolegend; 305806), and PECy5-CD45 (Clone: HI30, Biolegend; 304010) on ice for 30 min. Respective isotype controls were used to ensure minimal false positive background events. For the purposes of validating EC origin, PE-CD34 (Clone: 581, Biolegend; 343506), a pan-EC marker, was substituted for PE-CD106. After washing and suspension, the cells were then incubated with 7-Aminoactinomycin D (Biolegend; 420404) for analysis of cell viability. If FACS analysis was not performed immediately, cells were fixed in 1 % formaldehyde in FACS buffer. FACS analysis was performed at an event rate of 1,500 total events per second until 1×10^6 events were collected in a MNC gate that was based on characteristic forward scatter (FSC) and side scatter (SSC) properties. Data was acquired using CellQuest Software (Becton Dickinson, San Jose, CA, USA; 643436) and analysed using FlowJo analysis software (Treestar, Ashland, OR, USA). CD146 and VCAM-1 positivity were defined based on fluorescence intensity above FMO gating controls and that of the isotype IgG control antibody. CAECs were defined as FSC^{High} (indicating cells that are larger than noncellular particles for the purposes of eliminating contaminating platelets, non-viable cells, and EMPs), $CD45^-$ (non-leukocyte), and $CD146^+$. Activated CAECs were defined as FSC^{High}, $CD45^-$, $CD146^+$, and $VCAM\text{-}1^+$. Viability was assessed by 7-Aminoactinomycin D exclusion. MNCs were defined as FSC^{High} and $CD45^+$. Cell counts were computed by normalising the number of positive CAECs to the number of positive MNCs. VCAM-1 median fluorescence intensities (MFIs) were determined for the $VCAM\text{-}1^+$ CAEC subsets. VCAM-1 receptor number was obtained by converting MFIs to receptor binding sites using Quantum Simply Cellular Beads (Bangs Laboratories, Indianapolis, IN, USA), according to the manufacturer recommended protocol.

Whole blood lysate technique

For EMP analysis, 100 μl coronary artery blood was stained directly with AF488-CD146, PE-CD106, and the nucleic acid stain LDS-751 (Invitrogen, Carlsbad, CA, USA; L7595) for 30 min on ice. Each sample was lysed with 1 ml RBC lysis buffer (Biolegend; 420301) for 10 min. After centrifugation at 800g for 5 min, cells were resuspended with AccuCheck cell counting beads, possessing a defined concentration of reference beads, for the determination of absolute particle counts for sample comparison of CAEC and EMP number between subjects. Samples were standardised by collection of 20,000 AccuCheck cell counting beads. EMPs were defined as FSC-low (smaller in size than MNCs to eliminate analysis of CAECs) and $CD146^+$. Activated EMPs were defined as $VCAM\text{-}1^+$. RNA positivity was assessed by LDS-751 expression. EMP enumeration was performed using a single platform

absolute count with AccuCheck cell count beads. Absolute counts were determined by multiplying the numbers of acquired EMPs by a known concentration of counting beads as provided by the manufacturer and dividing by the number of acquired counting beads, according to the manufacturer recommended protocol.

HAEC culture

Cryopreserved human aortic ECs (HAECs) (Genlantis, San Diego, CA, USA; PH30405AK, Lot 2248) were used as positive EC biological controls, compensation controls, and in technique optimisation experiments. HAECs were expanded in 50 μg/ml rat tail collagen type 1-coated (BD Biosciences, Bedford, MA, USA) culture flasks. HAECs were grown in EC growth medium-2 (Lonza, Allendale, NJ, USA), supplemented with 10 % fetal bovine serum (Thermo Scientific – Hyclone, Waltham, MA, USA; CC-3162) and 1 % antibiotic-antimycotic solution (Invitrogen). HAECs were subcultured to 80–90 % confluence and used for experiments at passage 6 (16–19 total cell divisions). To quantitate VCAM-1 expression, HAECs were stimulated with tumour necrosis factor-α (TNFα) at a concentration of 0.3 ng/ml corresponding to the EC_{50} for maximal activation of expression (R&D Systems, Minneapolis, MN, USA; 210-TA-020) for 4 h, detached and harvested using 1 mM ethylenediaminetetraacetic acid dissociation buffer, as optimised and described previously (22).

Flow cytometry compensation

Unstained HAECs and AF488 CD146 single-stained HAECs were used as the AF488 compensation control. HAECs were labelled for 30 min on ice. For PE and PECy5 compensation controls, singlestained BD CompBeads (BD Biosciences; 552843) with appropriate fluorochromes were labelled according to manufacturer recommended protocol.

Amnis imaging flow cytometry

The Amnis FlowSight imaging flow cytometer was used to collect brightfield, darkfield (SSC) and fluorescent images of CAECs and HAECs for the purposes of validating EC phenotype (23). Twelve images per cell were captured at 20× magnification. The MNC isolation technique was used to prepare cells for imaging. Cells were fixed with 1 % formaldehyde. Prior to imaging flow cytometry (IFC) analysis, cells were incubated with 1 μg/ml DAPI on ice for 10 min. Images were acquired using Amnis INSPIRE software and fluorescence intensity and morphology were analysed using the Amnis IDEAS image analysis software. Multiple event files of 100,000 nucleated images were acquired and merged into one file to achieve 1x total MNC events.

The Amnis ImageStream^X imaging flow cytometer was used to collect brightfield and fluorescent images for the purposes of validating VCAM-1$^+$ CAECs. Six images per cell were captured at 40× magnification. PE-Texas Red CD45 (Clone: HI30, Molecular Probes, Eugene, OR, USA; MHCD4517), PECy7 CD146 (Clone: P1H12, BD Pharmingen; 562135) and PE-CD106 were used to image ECs on the Amnis. CellMask Deep Red (Life Technologies; C10046) was used to detect the cell plasma membrane. Prior to IFC analysis, cells were incubated with 1 μg/ml DAPI on ice for 10 min. Appropriate FMO controls were stained. Multiple event files of 100,000 nucleated images were acquired for practicality in

data size and merged into one file. CAECs were selected by gating for in-focus cells, $DAPI^+$ singlets, $CD45^-$, and $CD146^+$ at 10^6 total events. Viability was assessed by gating out events that demonstrated nuclear blebbing, as visible in DAPI images.

The details of VCAM-1^+ EC phenotype are shown by composite merged images of DAPI, CD146, and VCAM-1 in Suppl. Figure 2 (available online at www.thrombosis-online.com). CAECs were observed to exist as VCAM-1^- or VCAM-1^+ populations. Representative VCAM-1^+ CAECs and TNFα-activated HAECs are shown. Total $CD146^+$ CAECs were enumerated at a frequency of 0.1 % of the MNC population. VCAM-1^+ CAECs existed as 64 % of all CAECs. As a negative control, a healthy subject's peripheral blood was imaged on the ImageStream^X, yielding a CEC count of 0.01 % of the MNC population, with zero CECs showing positivity for VCAM-1 expression.

Delta centroid XY measurements were made to correlate cell sphericity with microparticle formation. The delta centroid XY is a compound feature that is comprised of the radial distance between the centroids of two roughly spherical geometries identified on an image in μm. CAECs demonstrating elongated, irregular geometries had a high delta centroid for CD146 and VCAM-1 relative to the location of the nucleus.

Determination of cell volume and VCAM-1 density

To acquire a standardized measure of VCAM-1 expression between CAECs, EMPs, CECs, and HAECs, we normalised its expression to cell volume and defined a VCAM-1 density measure. Cell volume was computed from measuring average cell diameter from IFC by drawing a mask around either the bright field image or CellMask membrane fluorescence. Assuming a spherical geometry, a ~4-fold greater volume was measured for HAECs compared to CAECs based on IFC, which was also confirmed by comparing the FSC-MFI quantified on the FACScan (Suppl. Figure 3, available online at www.thrombosis-online.com). To evaluate changes in CD146 expression as a function of volume for cells vs microparticles, we plotted CD146 vs FSC MFI and observed a direct relationship between the two parameters with a slope of ~2.0 (i.e. R^2=0.67), and this ratio was applied to compare VCAM-1 density between ECs and EMPs. Since we observed that a > 100-fold increase in VCAM-1 expression was accompanied by only a 20 % change in CD146 expression (Suppl. Figure 4, available online at www.thrombosis-online.com), we estimated VCAM-1 density according to the following equation:

$$\mathrm{VCAM-1Density} = \frac{VCAM-1_{Receptor\ Number}}{CD146_{Receptor\ Number}} \times \frac{CD146_{Receptor\ Number}}{FSC-MFI}$$

Statistical analysis

Data were analysed using GraphPad Prism Version 5 (GraphPad Software Inc., San Diego, CA, USA). CAEC number and VCAM-1 expression were compared between groups using the Mann-Whitney test for non-parametric data. Clinical demographics were compared between stable CAD and MI patients using Fisher's exact test. Comparisons in absolute count between patient peripheral blood CECs and coronary-derived CAECs were made

using the Wilcoxon matched pair test. Linear regression analysis comparing VCAM-1 receptor number and markers of myocardial necrosis was performed using Pearson coefficients. A multivariable model was also developed to assess the relationship between CAEC expression of VCAM-1 after adjusting for differences in patient baseline characteristics including age and baseline white blood cell count. P-values of < 0.05 were considered significant. All box and whisker data are plotted as 5th and 95^{th} percentile whiskers, 25th and 75th percentile boxes, and median values. All box plot data are plotted as the mean ± SEM.

Results

Isolation and identification of endothelial cells obtained during balloon angioplasty of coronary arteries

Balloon angioplasty at the site of atherosclerotic plaque causes local disruption and denudation of plaque ECs (18, 19, 24). We hypothesised that collection of coronary artery blood at the time of balloon angioplasty would enable isolation of ECs derived from the site of atherosclerotic plaque and provide a means of assessing inflammatory activation for individual patients. As part of clinical care in patients with stable CAD or MI, balloon angioplasty was performed prior to stent placement in 72 subjects (Table 1). Baseline patient demographics were similar between groups, including target lesion length and angiographic SYNTAX score. After diagnostic coronary angiography, a guiding catheter was advanced to the target vessel, and a wire was advanced past the lesion (Figure 1, upper right panel). A balloon was then advanced over the wire to the site of obstructive plaque (figure 1, lower right panel). The balloon was inflated against the endothelium at sufficient pressure to compress the plaque against the vessel wall and restore adequate blood supply downstream of the artery as part of routine clinical care. A blood sample containing the coronary angioplasty balloon residue as well as dislodged CAECs and cellular debris was aspirated through the catheter for collection immediately after balloon deflation. Initial analyses indicated that few cells remained adherent to the angioplasty balloon (~20 CAECs/ml), and that the majority of cells were dislodged into the surrounding coronary blood (~2,000 CAECs/ml) (Suppl. Figure 5, available online at www.thrombosis-online.com). We therefore focused subsequent analysis on the coronary artery blood aspirate obtained at the time of balloon angioplasty.

Circulating ECs in peripheral blood samples are comparatively rare relative to leukocytes and platelets, numbering 1–5 EC per 1,000 MNCs when assessed by flow cytometry (25–27). We reasoned that efficient analysis of rare cell events would require an enrichment step such as MNC collection on a Percoll density gradient, rather than analysis of intact cells after erythrocyte lysis. A comparison of EC detection between these techniques using stable CAD and MI coronary blood samples yielded a coefficient of variance for EC detection of ~5 % for the MNC enrichment technique (n=24), compared with a coefficient of variance of ~30 % for the erythrocyte lysis technique (n=18). We also compared the accuracy and reproducibility of both isolation techniques by spiking healthy control peripheral venous blood samples with TNFα-stimulated HAECs at a concentration of 1 HAEC per 1,000 MNCs, a ratio on par with that observed in clinical samples. The results, as shown in Table

2, demonstrate that MNC enrichment provides ~30-fold superior reliability in detection of rare EC events when compared to erythrocyte lysis of whole blood samples.

To detect CAECs in MNC-enriched blood samples, a hierarchical gating strategy was employed that involved exclusion of leukocytes and non-viable cells followed by identification of CAECs based on CD146 fluorescence, a surface protein expressed at cell junctions and the apical membrane of mature ECs (Figure 2) (28). A set of calibration beads was added to each sample at a defined concentration to ensure homogeneous sampling during acquisition and derive absolute cell counts. Detection of peripheral arterial blood ECs from the patients ranged from 30 ± 10 per 1,000 MNCs, which compared favorably with previous reports (Table 3) (29–32). By comparison, CD146 expressing CAECs isolated from coronary blood numbered between 70–150 per 1,000 MNCs. This three- to four-fold enrichment of CAECs in coronary blood relative to the peripheral circulation was also detected employing CD34, a second marker of EC lineage (33) (Suppl. Figure 6, available online at www.thrombosis-online.com).

It has previously been reported that patients with CAD have an increased number of peripheral blood circulating ECs compared to subjects without cardiovascular disease, but direct comparisons between dislodged coronary artery EC number among patients with stable CAD vs MI have not previously been reported (34–37). We therefore investigated whether the absolute numbers of CAECs recovered at the time of angioplasty could provide diagnostic value in discriminating between subjects with stable CAD versus those with MI. Evaluating 43 patients (stable CAD n=29, MI n=14) following angioplasty, we observed a mean relative CAEC count of 120 ± 30 per 1,000 MNCs for MI and 90 ± 20 for stable CAD subjects (p=0.3). Similarly, no significant difference in CAEC counts was found between samples based on a volumetric analysis of the aspirated blood between the stable CAD and MI patients (2,854 vs 2,283 cells/ml, p=0.4) (Figure 2D). In contrast, analysis of the circulating EC (CEC) in a subset of patients indicated a three- to four-fold increase in endothelial count between peripheral circulation and coronary arteries, (Suppl. Figure 7, available online at www.thrombosis-online.com, and Figure 2D). These results indicate that a similar number of ECs are disrupted at the site of coronary angioplasty, which markedly exceeds that in the peripheral circulation, regardless of whether the target lesion represents a stable or unstable plaque.

Myocardial infarction is associated with increased endothelial cell expression of VCAM-1

To address the hypothesis that MI elicits a significant increase in inflammatory activation of coronary artery plaque ECs, we next investigated the expression of VCAM-1 on CAECs and compared this with receptor expression on cultured HAECs stimulated with TNFα. Amnis IFC technology enabled measurement of fluorescence intensity along with detection of bright field images of cells in flight (23). A gating strategy was applied to identify viable ECs based on forward and side light scatter, absence of CD45 expression (a leukocyte marker), DAPI (nucleated), and CD146 expression (a mature endothelial marker) (Figure 3A). Composite merged images of DAPI, CD146, and VCAM-1 (Suppl. Figure 2, available online at www.thrombosis-online.com) revealed that CAECs were ~25 % the size of TNFα-activated HAECs, but on par with the size of CECs obtained from the peripheral circulation.

CAECs obtained from the coronary artery blood of patients with stable CAD and MI had higher VCAM-1 fluorescence compared with peripheral blood CECs, which were negative for VCAM-1 expression based on the fluorescence intensity of an IgG isotype control antibody. The number of CAECs that registered significant VCAM-1 expression vs total detected was not different between stable CAD and MI patients (Figure 3B). In contrast, histograms of fluorescence of CAECs confirmed a right shift in VCAM-1 fluorescence separating MI from stable CAD patients (Figure 3C). Among the CAECs positive for VCAM-1, the average receptor number expressed in patients with MI was 73 % higher than for patients with stable CAD ($p=0.01$) (Figure 3D). These results were unchanged after adjusting for differences between patient baseline age and white blood cell count ($p=0.01$). Moreover, we found no significant correlation between post-procedure myocardial blush or corrected TIMI frame count and endothelial cell VCAM-1 expression among patients with myocardial infarction, suggesting that endothelial VCAM-1 levels were not associated with markers of myocardial perfusion. In contrast, virtually all HAECs stimulated with TNFα exhibited strong fluorescence expression for VCAM-1, registering up to 1.5×10^6 receptors per HAEC (Figure 3D). These data suggest that MI is associated with more highly activated CAECs at the site of plaque disruption and that receptor expression level corresponding to EC inflammation detected ex vivo is orders of magnitude less than that of TNFα-stimulated HAECs under cell culture conditions.

Coronary artery endothelial microparticles upregulate VCAM-1 during myocardial infarction

EMPs are pro-thrombotic, pro-coagulant, and pro-inflammatory, suggesting a pathologic role in vascular disorders (5, 38, 39). Providing evidence for the release of EMPs at the plaque site was the observation of CAECs with elongated, irregular geometries with positive expression for CD146 and VCAM-1 detected on portions of plasma membrane that were stretched from the nucleus (Figure 3A). Analysis using the delta centroid XY feature on Amnis IDEAS software that provided spatial discrimination between DAPI and VCAM-1 signals, revealed that 48 % of the VCAM-1 expressed on CAECs was nonuniformly distributed on the membrane. Taken together, this provides circumstantial evidence implicating VCAM-1 enriched EMPs are derived from CAEC obtained at the site of plaque disruption.

We next examined the levels of coronary artery-derived EMPs following angioplasty and whether EMP expression of VCAM-1 discriminated the relative inflammatory status of stable CAD and MI subjects. Peripheral and coronary artery blood samples were assessed for formation of EMPs, which were identified by their characteristic low forward scatter intensity, consistent with their volume being an order of magnitude smaller than that of leukocytes (Figure 4A). EMPs also were observed to express CD 146 and a fraction co-expressed VCAM-1 (Figure 4B, C). Similar to CAEC number, no significant difference was observed in overall EMP counts between stable CAD and MI patients (Suppl. Figure 8, available online at www.thrombosis-online.com). However, EMP count was elevated in coronary arteries vs peripheral circulation when compared in matched blood samples from individual patients (Suppl. Figure 7, available online at www.thrombosis-online.com). Distinct from CEC, which did not express measurable VCAM-1 receptor, significant levels

were detected on peripheral blood EMPs. Moreover, the fraction of VCAM-1^+ EMP was significantly greater in MI than stable CAD (Figure 4D ; 24.9 ± 2.7%, vs 13.9 ± 1.2 %, p=0.007), and for each patient the level consistently increased between peripheral and coronary artery matched blood samples (Suppl. Figure 7, available online at www.thrombosis-online.com). Taken together, these findings indicate that VCAM-1 expression on circulating EMPs represents a biologically important marker of arterial inflammation.

To further assess VCAM-1 expression and attempt to discriminate the inflammatory status of patients, we quantified VCAM-1 density on EMPs and intact CAECs. Particle and cell volume were analysed by forward scatter intensity, which revealed a wide size range: EMP volume was estimated at 80 μm^3, stable CAD and MI CAEC volume averaged 700 μm^3, and HAEC volume averaged 3,300 μm^3 based on measurement of spherical diameters quantified from IFC images (Figure 5A). The relative density of VCAM-1 on CAEC vs EMPs was determined by measuring the ratio of CD146 to forward scatter. IFC revealed that VCAM-1 density was ~1-fold higher on CAECs from MI than stable CAD subjects (Figure 5B). A remarkable observation was that the density of VCAM-1 on EMPs was ~5-fold higher than on CAECs. This analysis also revealed that *in-vitro* TNFα-stimulated HAECs express ~20-fold higher VCAM-1 density compared to activated CAECs detected *ex vivo*.

Coronary artery endothelial and microparticle VCAM-1 density correlates with myocardial infarct size

There is wide variability in clinical presentation with MI, and larger infarcts may be associated with greater inflammation at the level of the coronary artery plaque and subtended myocardium. VCAM-1 receptor density on CAECs was significantly higher for patients with larger myocardial infarct size, as determined by peak levels of creatine kinase ($p< 0.01$) and troponin levels in serum ($p< 0.01$). By comparison, MI patients with lower levels of these biomarkers had CAEC VCAM-1 density similar to that of patients with stable CAD (Figure 5C).

Discussion

Prediction and identification of plaque rupture remains a central challenge in cardiology. Better understanding the biology of endothelium directly at the site of atherosclerotic plaque could lead to new interventions that interrupt local inflammatory pathways and predict subsequent plaque healing and stability. Although both stable CAD and MI are associated with systemic inflammation, we reasoned that differences in the number or inflammatory state of coronary artery plaque endothelium would correlate with disease presentation. To test this hypothesis, a conventional FACScan flow cytometer was used to analyse CAECs collected from catheter blood samples immediately after balloon angioplasty. We found that the overall number of CAECs harvested from coronary blood did not discriminate between subjects with stable CAD vs MI. However, CAECs from MI patients registered ~1-fold higher VCAM-1 expression relative to patients with stable CAD. In contrast, VCAM-1 was undetectable on intact CEC from the peripheral circulation. Direct visualisation of CAEC morphology employing IFC revealed that a significant number exhibited an irregular

geometry when compared with more spherically symmetric circulating ECs and HAECs. This altered geometry portended the formation of EMPs that expressed 10-fold higher density of VCAM-1 than on intact cells, and like CAECs were observed in greater numbers in patients with MI than with stable CAD. A distinct difference from CEC, was that VCAM-1$^+$ EMPs were observed in the peripheral arteries of MI and CAD subjects. Biomarkers of MI severity, including serum creatine kinase and troponin, were elevated to a greater extent in the patients whose CAECs registered the highest VCAM-1 density. By sampling catheter blood collected during angioplasty and using flow cytometric analysis, we provide direct evidence that local EC activation can be assessed based on the relative membrane expression of VCAM-1 on coronary artery plaque endothelium and EMPs.

VCAM-1 as a biomarker of coronary artery plaque inflammation

VCAM-1 plays a central role in leukocyte recruitment to both nascent and established atherosclerotic plaque (40–42). Consistent with this pathophysiologic role, inflammatory cytokines and circulating (i.e. membrane shed) EC adhesion receptors are associated with a number of adverse cardiovascular outcomes, including an increased risk of cardiovascular death among patients with established CAD (43). Because prior studies have relied on circulating levels of soluble VCAM-1, little is known about VCAM-1 expression and inflammation directly at the site of coronary artery plaque. Our study is the first direct observation that VCAM-1 is upregulated on EMPs and CAECs. Importantly, in every case of CAD and MI we observed elevated levels of VCAM-1 expression on coronary EMPs compared to the peripheral blood. Our studies provide a method for evaluating coronary artery endothelial activation based on relative VCAM-1 expression, as validated by fluorescence imaging. Our data also suggest that upregulation of VCAM-1 is a risk factor for plaque instability leading to MI and may also contribute to the elevated inflammatory response during MI.

We observed relatively low levels of VCAM-1 expression on CAECs as compared to TNFα-stimulated HAECs. This was due in part to a marked difference in cell volume of HAECs, which exceeded CAECs by up to ~4-fold. Even after accounting for this difference, HAECs still expressed ~20-fold higher density of VCAM-1 compared with CAECs. Several factors may account for the lower level of VCAM-1 on CAECs. First, HAECs in culture may have altered response to TNFα activation. Second, persistent inflammation at the site of atherosclerotic plaque may promote shedding of VCAM-1 from the endothelial membrane, either as soluble VCAM-1 or enriched on EMP that are shed from EC following plaque disruption. Consistent with this hypothesis, we found that EMPs had approximately 10-fold greater VCAM-1 density compared to CAECs. Imminent formation of EMPs was apparent from direct observation of morphology by IFC, in which bright field images often revealed irregularly shaped CAECs containing membrane tethers, as well as dense anti-VCAM-1 labelling of the EMPs (Suppl. Figure 2, available online at www.thrombosis-online.com). It has been reported that EMPs are shed as a result of cell activation, vessel injury, or cell death. This is the first report of a hierarchy in VCAM-1 density and suggests that VCAM-1 may provide a dynamic biomarker that reports on the process of liberation of ECs and EMPs from atherosclerotic lesions. These fragments may play a role in plaque formation and

vessel occlusion, as EMPs are procoagulant, thereby increasing the likelihood of atherothrombosis and MI (45).

Detection of rare event endothelial cells in whole blood samples

ECs within the systemic circulation are rare cells that are commonly assumed to be a surrogate marker for endothelial dysfunction (45). Previous studies have reported positive correlations between increased CEC counts and cardiovascular diseases. A wide range in the count of circulating ECs can be found in the literature, ranging from 0 to 39,100 cells/ml in patients with vascular disorders and from 0 to 7,900 in healthy controls (33). We observed similar peripheral arterial blood circulating EC count numbers for patients with CAD vs MI using flow cytometry. To arrive at a standardised technique for discrimination of rare event CAECs from catheter samples during coronary artery balloon angioplasty, we compared two techniques for CAEC identification and enumeration – MNC isolation and whole blood lysis. The MNC isolation technique was selected for CAEC analysis and its accuracy was confirmed in whole blood HAEC-spiking experiments using CD146 for identification, a glycoprotein involved in cell-cell adhesion (46) and expressed on mature ECs (47). The RNA dye LDS-751 was also employed to assess RNA-positivity of the EMPs, which has previously been reported (5, 14). Utilisation of this technique resulted in reproducible rare cell event isolation while minimising false positive events.

Endothelial microparticles and myocardial injury

EMPs are released by activated or apoptotic ECs. By using a gradient isolation technique and avoiding a red blood cell lysis step, we succeeded in the enrichment of EC and EMP for subsequent analysis. Prior studies have reported that patients with MI have increased coronary artery levels of EMPs compared with circulating levels (10, 48, 49). One of these studies reported an inverse association between coronary EMP levels and myocardial perfusion grade, suggesting that coronary EMP levels are associated with microvascular obstruction (10). Notably, that study utilised blood obtained during the initial thrombus aspiration, rather than after balloon angioplasty. Although we did not find differences in the number of coronary plaque-derived EMPs between patients with stable CAD vs MI, VCAM-1^+ EMPs composed a significantly higher percentage of total EMPs and revealed a hierarchy in inflammation greatest in coronary arteries of patients with MI. Our findings of similar overall CAEC and EMP number between MI and stable CAD after angioplasty, coupled with increased VCAM-1 expression on EMPs suggest that activated CAECs from patients with MI are prone to breaking into similarly-activated cell fragments. Interestingly, the relative enrichment of VCAM-1 (approximately 10-fold) on EMPs compared to intact CAECs suggests that areas of intact ECs with a greater density of VCAM-1 may be more prone to EMP vesicle formation. Future studies will further investigate the mechanisms of EMP formation in MI and the role of activated EMPs in monocyte recruitment and lateral signalling to proximal ECs in coronary arteries.

Utility of VCAM-1 expression on CAECs and EMPs as a prognostic tool

Dissection of the local inflammatory pathways that occur directly at the site of coronary plaque promise a better understanding of local plaque biology and the mechanisms leading to plaque instability. In this study, VCAM-1 density on CAEC correlated with markers of

myocardial injury (e. g. peak CK, peak troponin) for MI patients, as stable CAD patients do not typically register detectable levels of these markers. Given the range of VCAM-1 receptor density expressed on CAECs and EMPs, it is possible that this marker may have prognostic significance for a given patient's future risk of recurrent cardiovascular events. The intensity of VCAM-1 upregulation on EMPs may also identify different underlying mechanisms leading to MI, such as plaque rupture vs erosion. Additional studies are warranted to investigate the utility of coronary artery endothelial VCAM-1 levels as a predictor of adverse outcomes after MI, and to determine the biological mechanisms responsible for local up-regulation of EMP formation leading to VCAM-1 enrichment.

Supplementary Material

Refer to Web version on PubMed Central for supplementary material.

Acknowledgements

We thank Christine Probst, applications scientist for Amnis, for her expertise in IFC data acquisition and analysis via IDEAS software. We also thank Dr. Mary Baldwin for assistance with drawing Figure 1. We would also like to thank the patients who consented to participate in the study.

Financial support:

This study was made possible with assistance from AHA 11CRP7260031 Clinical Research Program, NIH RO1 HL082689, and the University of California San Francisco-Gladstone Institute of Virology & Immunology Center for AIDS Research (CFAR), an NIH-funded program (P30AI027763).

References

1. Heidenreich PA, Trogdon JG, Khavjou OA, et al. Forecasting the future of cardiovascular disease in the United States: a policy statement from the American Heart Association. Circulation. 2011; 123:933–944. [PubMed: 21262990]
2. Roger VL, Go AS, Lloyd-Jones DM, et al. Heart disease and stroke statistics--2012 update: a report from the American Heart Association. Circulation. 2012; 125:e2–e220. [PubMed: 22179539]
3. Cannon CP, Weintraub WS, Demopoulos LA, et al. Comparison of early invasive and conservative strategies in patients with unstable coronary syndromes treated with the glycoprotein IIb/IIIa inhibitor tirofiban. New Engl J Med. 2001; 344:1879–1887. [PubMed: 11419424]
4. Schwartz GG, Olsson AG, Ezekowitz MD, et al. Myocardial Ischemia Reduction with Aggressive Cholesterol Lowering Study, Effects of atorvastatin on early recurrent ischemic events in acute coronary syndromes: the MIRACL study: a randomized controlled trial. J Am Med Assoc. 2001; 285:1711–1718.
5. Curtis AM, Edelberg J, Jonas R, et al. Endothelial microparticles: sophisticated vesicles modulating vascular function. Vasc Med. 2013; 18:204–214. [PubMed: 23892447]
6. Bonetti PO, Lerman LO, Lerman A. Endothelial dysfunction: a marker of atherosclerotic risk. Arterioscl Thromb Vasc Biol. 2003; 23:168–175. [PubMed: 12588755]
7. Davignon J, Ganz P. Role of endothelial dysfunction in atherosclerosis. Circulation. 2004; 109:III27–III32. [PubMed: 15198963]
8. Ross R. Atherosclerosis--an inflammatory disease. New Engl J Med. 1999; 340:115–126. [PubMed: 9887164]
9. Kinlay S, Ganz P. Role of endothelial dysfunction in coronary artery disease and implications for therapy. Am J Cardiol. 1997; 80:11I–16I. [PubMed: 9205012]
10. Porto I, Biasucci LM, De Maria GL, et al. Intracoronary microparticles and microvascular obstruction in patients with ST elevation myocardial infarction undergoing primary percutaneous intervention. Eur Heart J. 2012; 33:2928–2938. [PubMed: 22453653]

11. Zamani P, Schwartz GG, Olsson AG, et al. Myocardial Ischemia Reduction with Aggressive Cholesterol Lowering Study, Inflammatory biomarkers, death, and recurrent nonfatal coronary events after an acute coronary syndrome in the MIRACL study. J Am Heart Assoc. 2013; 2:e003103. [PubMed: 23525424]
12. Malek AM, Alper SL, Izumo S. Hemodynamic shear stress and its role in atherosclerosis. J Am Med Assoc. 1999; 282:2035–2042.
13. DePaola N, Gimbrone MA, Davies PF, et al. Vascular endothelium responds to fluid shear stress gradients. Arterioscl Thromb. 1992; 12:1254–1257. [PubMed: 1420084]
14. van der Heyde HC, Gramaglia I, Combes V. Flow cytometric analysis of micro-particles. Methods Mol Biol. 2011; 699:337–354. [PubMed: 21116991]
15. Steppich B, Mattisek C, Sobczyk D, et al. Ott, Tissue factor pathway inhibitor on circulating microparticles in acute myocardial infarction. Thromb Haemost. 2005; 93:35–39. [PubMed: 15630488]
16. Leroyer AS, Tedgui A, Boulanger CM. Role of microparticles in atherothrombosis. J Int Med. 2008; 263:528–537.
17. Diamant M, Tushuizen ME, Sturk A, et al. Cellular microparticles: new players in the field of vascular disease? Eur J Clin Invest. 2004; 34:392–401. [PubMed: 15200490]
18. Feng L, Stern DM, Pile-Spellman J. Human endothelium: endovascular biopsy and molecular analysis. Radiology. 1999; 212:655–664. [PubMed: 10478228]
19. Yu SY, Song YM, Li AM, et al. Isolation and characterisation of human coronary artery-derived endothelial cells in vivo from patients undergoing percutaneous coronary interventions. J Vasc Res. 2009; 46:487–494. [PubMed: 19204406]
20. Gibson CM, Cannon CP, Murphy SA, et al. Relationship of TIMI myocardial perfusion grade to mortality after administration of thrombolytic drugs. Circulation. 2000; 101:125–130. [PubMed: 10637197]
21. Gibson CM, Cannon CP, Daley WL, et al. TIMI frame count: a quantitative method of assessing coronary artery flow. Circulation. 1996; 93:879–888. [PubMed: 8598078]
22. Ting HJ, Stice JP, Schaff UY, et al. Triglyceride-rich lipoproteins prime aortic endothelium for an enhanced inflammatory response to tumor necrosis factor-alpha. Circ Res. 2007; 100:381–390. [PubMed: 17234968]
23. Samsel L, Dagur PK, Raghavachari N, et al. Imaging flow cytometry for morphologic and phenotypic characterisation of rare circulating endothelial cells. Cytometry B. 2013; 84:379–389.
24. Mutin M, Canavy I, Blann A, et al. Direct evidence of endothelial injury in acute myocardial infarction and unstable angina by demonstration of circulating endothelial cells. Blood. 1999; 93:2951–2958. [PubMed: 10216090]
25. Del Papa N, Colombo G, Fracchiolla N, et al. Circulating endothelial cells as a marker of ongoing vascular disease in systemic sclerosis. Arthritis Rheumatism. 2004; 50:1296–1304. [PubMed: 15077314]
26. Mancuso P, Antoniotti P, Quarna J, et al. Validation of a standardized method for enumerating circulating endothelial cells and progenitors: flow cytometry and molecular and ultrastructural analyses. Clin Cancer Res. 2009; 15:267–273. [PubMed: 19118054]
27. Mund JA, Estes ML, Yoder MC, et al. Flow cytometric identification and functional characterisation of immature and mature circulating endothelial cells. Arterioscl Thromb, Vasc Biol. 2012; 32:1045–1053. [PubMed: 22282356]
28. Bardin N, Anfosso F, Masse JM, et al. Identification of CD146 as a component of the endothelial junction involved in the control of cell-cell cohesion. Blood. 2001; 98:3677–3684. [PubMed: 11739172]
29. Estes ML, Mund JA, Ingram DA, et al. Identification of endothelial cells and progenitor cell subsets in human peripheral blood. In: Current protocols in cytometry. 2010
30. Solovey A, Lin Y, Browne P, et al. Circulating activated endothelial cells in sickle cell anemia. N Engl J Med. 1997; 337:1584–1590. [PubMed: 9371854]
31. Kas-Deelen AM, de Maar EF, Harmsen MC, et al. Uninfected and cytomegalic endothelial cells in blood during cytomegalovirus infection: effect of acute rejection. J Infectious Dis. 2000; 181:721–724. [PubMed: 10669362]

32. Mutunga M, Fulton B, Bullock R, et al. Circulating endothelial cells in patients with septic shock. Am J Resp Crit Care Med. 2001; 163:195–200. [PubMed: 11208646]
33. Kraan J, Strijbos MH, Sieuwerts AM, et al. A new approach for rapid and reliable enumeration of circulating endothelial cells in patients. J Thromb Haemost. 2012; 10:931–939. [PubMed: 22385979]
34. Makin AJ, Blann AD, Chung NA, et al. Assessment of endothelial damage in atherosclerotic vascular disease by quantification of circulating endothelial cells Relationship with von Willebrand factor and tissue factor. Eur Heart J. 2004; 25:371–376. [PubMed: 15033248]
35. Boos CJ, Lip GY, Blann AD. Circulating endothelial cells in cardiovascular disease. J Am Coll Cardiol. 2006; 48:1538–1547. [PubMed: 17045885]
36. Damani S, Bacconi A, Libiger O, et al. Characterisation of circulating endothelial cells in acute myocardial infarction. Science Transl Med. 2012; 4:126ra133.
37. Lee KW, Lip GY, Tayebjee M, et al. Circulating endothelial cells, von Willebrand factor, interleukin-6, and prognosis in patients with acute coronary syndromes. Blood. 2005; 105:526–532. [PubMed: 15374879]
38. Combes V, Simon AC, Grau GE, et al. In vitro generation of endothelial micro-particles and possible prothrombotic activity in patients with lupus anticoagulant. J Clin Invest. 1999; 104:93–102. [PubMed: 10393703]
39. Bombeli T, Karsan A, Tait JF, et al. Apoptotic vascular endothelial cells become procoagulant. Blood. 1997; 89:2429–2442. [PubMed: 9116287]
40. Iiyama K, Hajra L, Iiyama M, et al. Patterns of vascular cell adhesion molecule-1 and intercellular adhesion molecule-1 expression in rabbit and mouse atherosclerotic lesions and at sites predisposed to lesion formation. Circ Res. 1999; 85:199–207. [PubMed: 10417402]
41. Li H, Cybulsky MI, Gimbrone MA, et al. Inducible expression of vascular cell adhesion molecule-1 by vascular smooth muscle cells in vitro and within rabbit atheroma. Am J Path. 1993; 143:1551–1559. [PubMed: 7504883]
42. Libby P, Li H. Vascular cell adhesion molecule-1 and smooth muscle cell activation during atherogenesis. J Clin Invest. 1993; 92:538–539. [PubMed: 7688759]
43. Blankenberg S, Rupprecht HJ, Bickel C, et al. Circulating cell adhesion molecules and death in patients with coronary artery disease. Circulation. 2001; 104:1336–1342. [PubMed: 11560847]
44. Shantsila E, Kamphuisen PW, Lip GY. Circulating microparticles in cardiovascular disease: implications for atherogenesis and atherothrombosis. J Thromb Haemost. 2010; 8:2358–2368. [PubMed: 20695980]
45. Blann AD, Woywodt A, Bertolini F, et al. Circulating endothelial cells Biomarker of vascular disease. Thromb Haemost. 2005; 93:228–235. [PubMed: 15711737]
46. Lehmann JM, Riethmuller G, Johnson JP. MUC18, a marker of tumor progression in human melanoma, shows sequence similarity to the neural cell adhesion molecules of the immunoglobulin superfamily. Proc Natl Acad Sci USA. 1989; 86:9891–9895. [PubMed: 2602381]
47. Strijbos MH, Kraan J, den Bakker MA, et al. Cells meeting our immunophenotypic criteria of endothelial cells are large platelets. Cytometry B. 2007; 72:86–93.
48. Morel O, Pereira B, Averous G, et al. Increased levels of procoagulant tissue factor-bearing microparticles within the occluded coronary artery of patients with ST-segment elevation myocardial infarction: role of endothelial damage and leukocyte activation. Atherosclerosis. 2009; 204:636–641. [PubMed: 19091315]
49. Min PK, Kim JY, Chung KH, et al. Local increase in microparticles from the aspirate of culprit coronary arteries in patients with ST-segment elevation myocardial infarction. Atherosclerosis. 2013; 227:323–328. [PubMed: 23422831]

What is known about this topic?

- Plaque stability is influenced by multiple inflammatory pathways, but direct assessment of endothelial inflammation at the site of coronary artery stenosis in humans has been limited to pathology samples or animal models of atherosclerosis.
- Both circulating VCAM-1 level and endothelial microparticle number have been associated with increased risk of adverse outcomes after MI, but no studies have reported the levels of plaque VCAM-1 expression or the relationship of endothelial activation to microparticle formation.

What does this paper add?

- A novel flow cytometric based technique was applied to quantify coronary artery endothelial cell and microparticle expression of VCAM-1 from coronary plaque samples of patients with stable CAD or MI undergoing balloon angioplasty.
- Coronary endothelium from MI patients registered higher expression of VCAM compared to patients with stable CAD and formed microparticles that expressed 10-fold higher density of VCAM-1 than on intact cells.

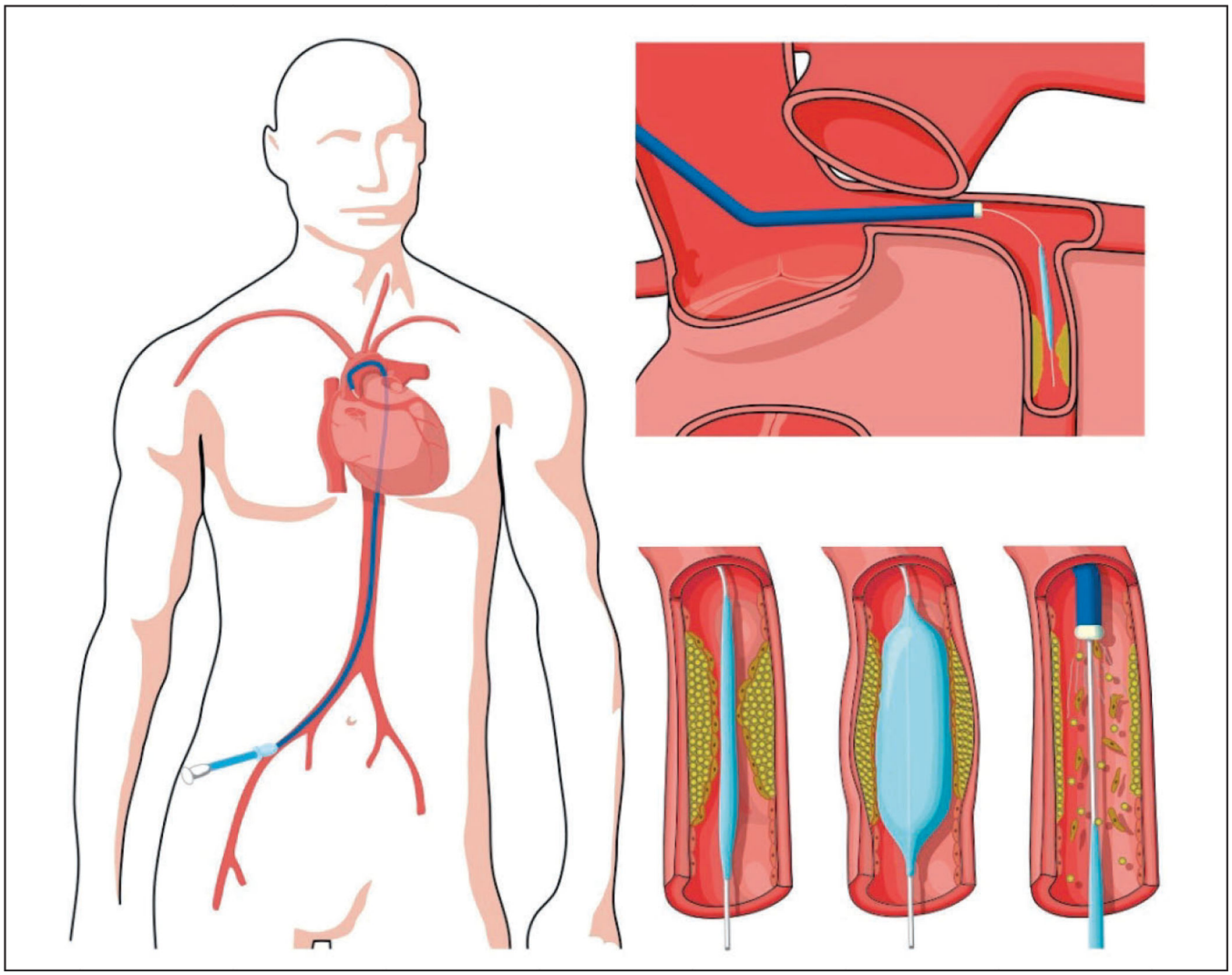

Figure 1. Isolation of human coronary artery endothelial cells from sites of atherosclerotic plaque

Left panel: a catheter is advanced through the femoral artery to the origin of the coronary artery. Selective coronary angiography is then performed using injection of radiopaque contrast. Upper right panel: A wire is advanced through this guide catheter into the coronary artery past the site of obstruction. Lower right panel: A balloon is advanced over the wire to the site of an obstructive coronary artery plaque. The balloon is expanded to compress the plaque. During the angioplasty process, endothelial cells become dislodged into the blood. The balloon is deflated, and blood surrounding the balloon is immediately aspirated, from the guide catheter. Flow cytometry analysis is performed on the retrieved coronary artery blood (Adapted from Baim DS: Percutaneous balloon angioplasty and general coronary intervention. In: Baim DS: Grossman's Cardiac Catheterization, Angiography, and Intervention, 7th ed. Philadelphia, Lippincott Williams & Wilkins, 2005 and http://qualitycardiaccare.com).

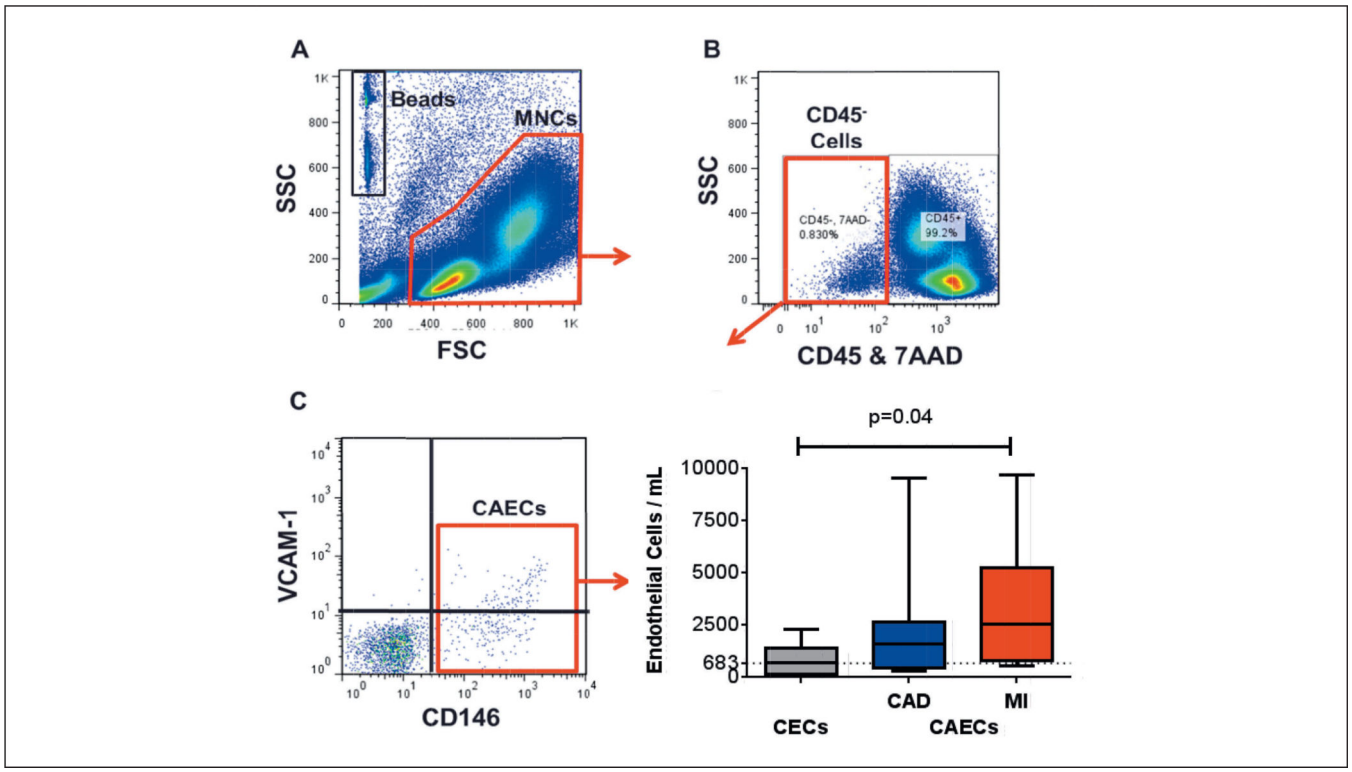

Figure 2. Identification of coronary artery ECs (CAECs) and human aortic ECs (HAECs) by flow cytometry

A) CAECs were identified by FACS using a hierarchical gating strategy. Cells within a mononuclear cell (MNC) region were first identified by forward scatter (FSC) and side scatter (SSC). AccuCheck counting beads (top left corner) were used to ensure homogeneous sampling during acquisition. B) Cells lacking expression of CD45- (non-leukocyte, to eliminate CD146+ activated T-lymphocytes) and 7-AAD-(viable) cells were selected. C) CAECs were identified as CD45/7-AAD^{-}/CD146^{+} events. Mean fluorescence expression of VCAM-1 (y-axis) above FMO control was used to assess EC activation. D) Absolute cell counts were enumerated to compare numbers of endothelial cells per ml of blood for stable CAD (2,283 ± 688 CAECs/ml (mean ± SEM), n=14) and MI (2,854 ± 1,093 CAECs/ml, n=8) patient CAEC and peripheral arterial blood circulating endothelial cell (CEC) (626 ± 236 CECs/ml, n=5). MI CAEC absolute count was significantly increased compared to patient peripheral CEC controls (p=0.04; Mann-Whitney test). Stable CAD CAEC absolute count approached significance compared to CEC controls (p=0.07; Mann-Whitney test). Absolute counts between patients with stable CAD and MI showed no significant difference (p=0.4; Mann-Whitney test). Box and whisker plot shows 5th and 95th percentile whiskers, 25th and 75th percentile boxes and mean values.

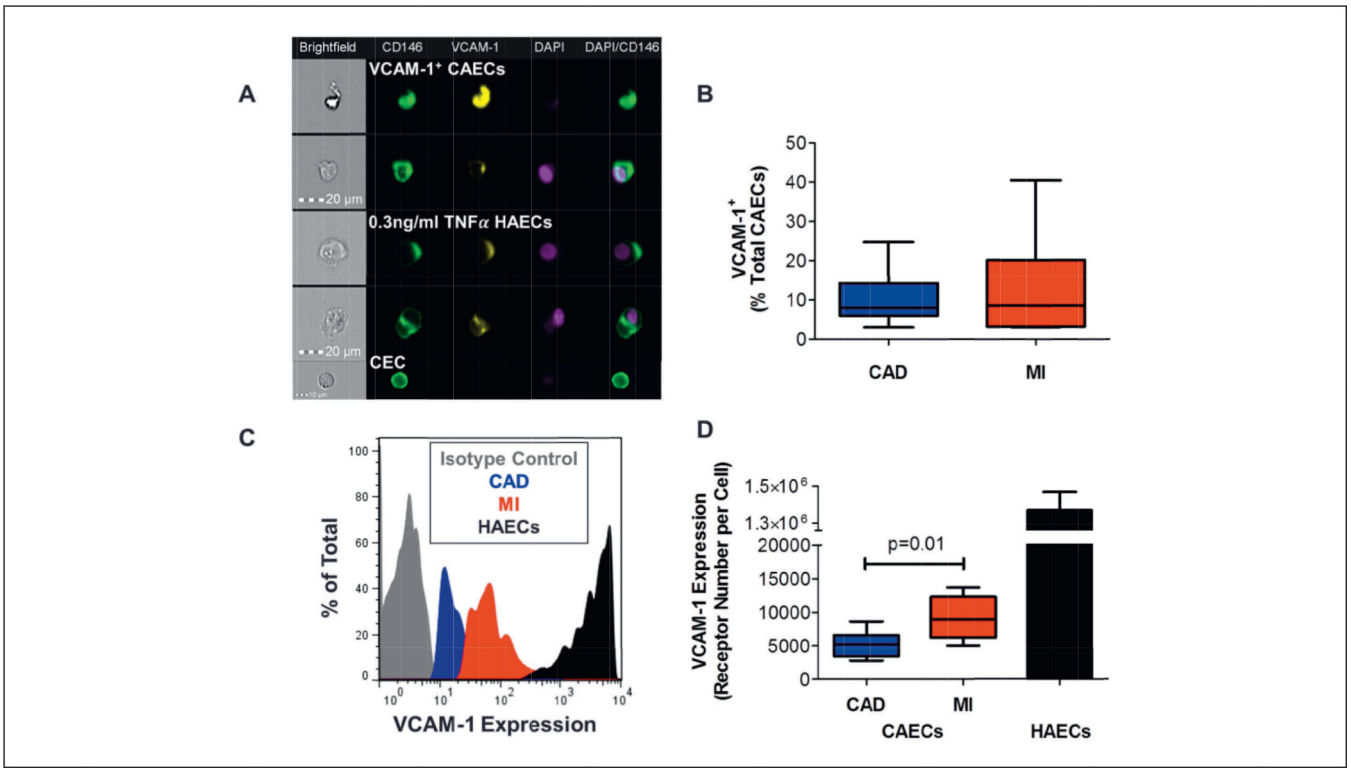

Figure 3. VCAM-1 expression on endothelial cells

A) Bright field and fluorescent images of VCAM-1 on ECs using imaging flow cytometry (IFC) at 20× magnification (Representative images from n=3 separate experiments). CAECs were $DAPI^+$ (nucleated), $CD146^+$ (endothelial origin), $CD45^-$ (non-leukocyte, not shown), and viable (based on a lack of nuclear blebbing). Activated CAECs were $VCAM\text{-}1^+$, while peripheral blood CECs were uniformly VCAM-1. Representative IFC images are shown for human aortic endothelial cells (HAECs) stimulated with TNF at 0.3 ng/ml (EC_{50} for maximal stimulation). CAECs and HAECs were similar in phenotype: $DAPI^+$, $CD45^-$, $CD146^+$, and $VCAM\text{-}1^+$. CAECs within clinical samples were observed to exist as either $VCAM\text{-}1^-$ or $VCAM\text{-}1^+$. When activated they often displayed characteristic membrane blebs with uniform expression of CD146 and VCAM-1. B) The proportion of $VCAM\text{-}1^+$ CAECs (% total CD146 positive) was not significantly different between stable CAD (10.7 ± 1.7 % (mean ± SEM), n=13) and MI (14 ± 5.2 %, n=7) patient subsets (p=0.8; Mann-Whitney test). Furthermore, $VCAM\text{-}1^+$ EC count was not significantly different between stable CAD (268 ± 138 cells / ml, n=13) and MI (263 ± 121 cells / ml, n=7) patient subsets (p=0.5; Mann-Whitney test). Box and whisker plot 5th and 95th percentile whiskers, 25th and 75th percentile boxes, and median values. C) Fluorescence histograms of VCAM-1 for $VCAM\text{-}1^+$ CAECs for a stable CAD patient (50 cells) and an MI patient (67 cells) reveal a positive shift in VCAM-1 MFI for the MI sample. Comparison to VCAM-1 expression on respective PE-conjugated IgG isotype controls indicates positive, specific VCAM-1 expression on clinical samples. TNFα-stimulated human aortic endothelial cells (HAECs) express greater VCAM-1 relative to patient samples. D) Among $VCAM\text{-}1^+$ CAECs, patients with MI had a significantly higher expression of VCAM-1 (9,004 ± 1,226 receptors per cell) compared to patients with stable CAD (5,123 ± 494 receptors per cell) (p=0.01; Mann-

Whitney test). As HAECs are much larger, these ECs exhibited significantly higher VCAM-1 expression ($1.3\times10^6 \pm 122{,}000$ receptors per cell). Box and whisker plot shows 5th and 95th percentile whiskers, 25th and 75th percentile boxes, and median values.

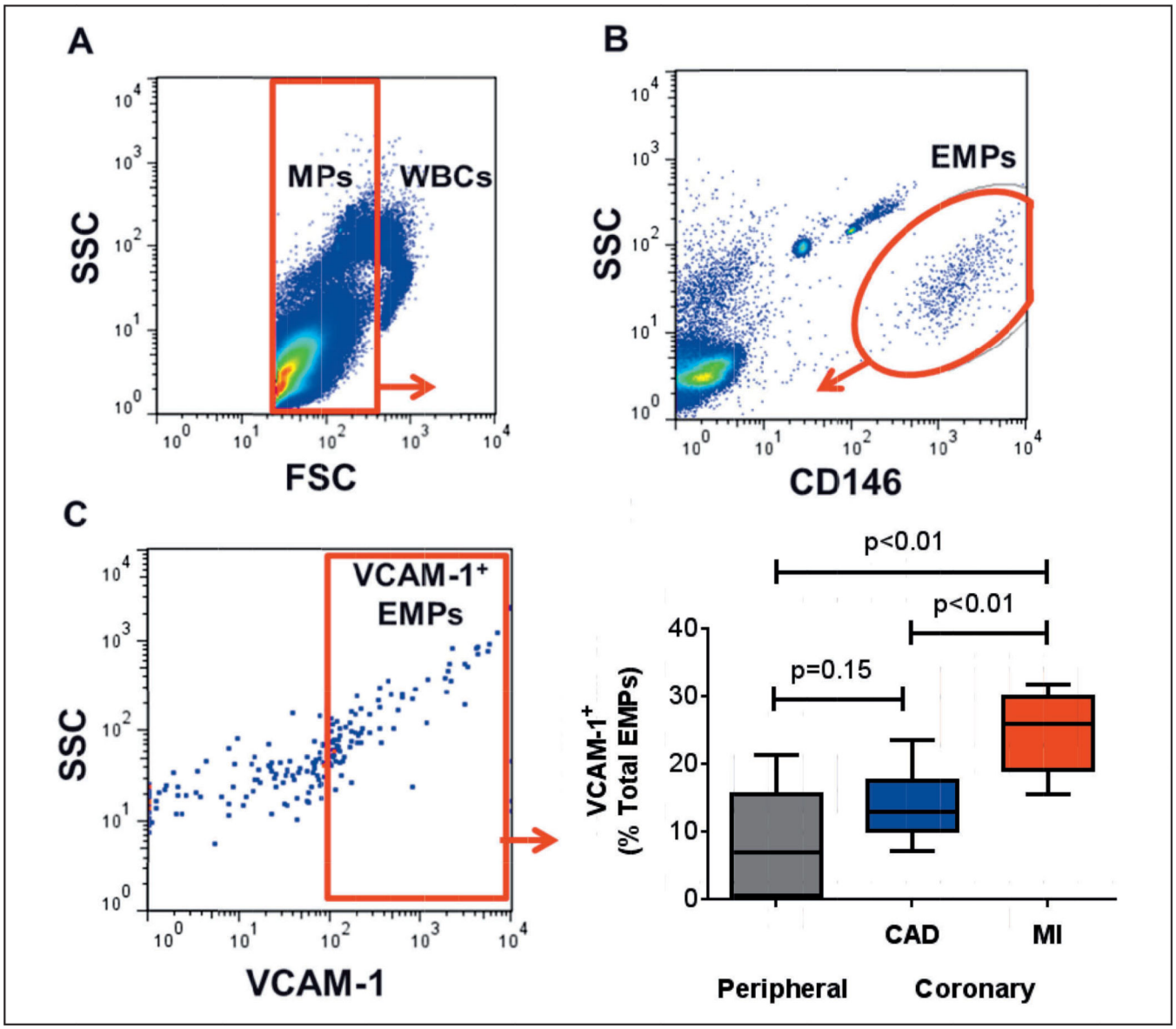

Figure 4. Identification of coronary artery endothelial cell-derived microparticles (EMPs)

A) Non-cellular microparticles (MPs) are identified as low FSC (FSCLow) compared with white blood cells (WBCs). B) FSCLow particles are identified as CD146$^+$ EMPs. C) A representative MI patient's EMPs are shown within a SSC vs VCAM-1 bivariate dot plot. The box gate on VCAM-1$^+$ EMP was assigned based on a 100-channel threshold identified from the expression of non-stimulated HAEC control. D) Measurements of VCAM-1$^+$ EMPs (% total EMPs) for patients with stable CAD (13.9 ± 1.2 % (mean ± SEM), n=15) was significantly lower than for patients with MI (24.9 ± 2.7 %, n=5) ($p \leq 0.01$; Mann-Whitney test). The percentage of VCAM-1$^+$ EMPs in coronary artery blood was also higher for patients with CAD and MI compared to peripheral blood. Box and whisker plot shows 5th and 95th percentile whiskers, 25th and 75th percentile boxes, and median values.

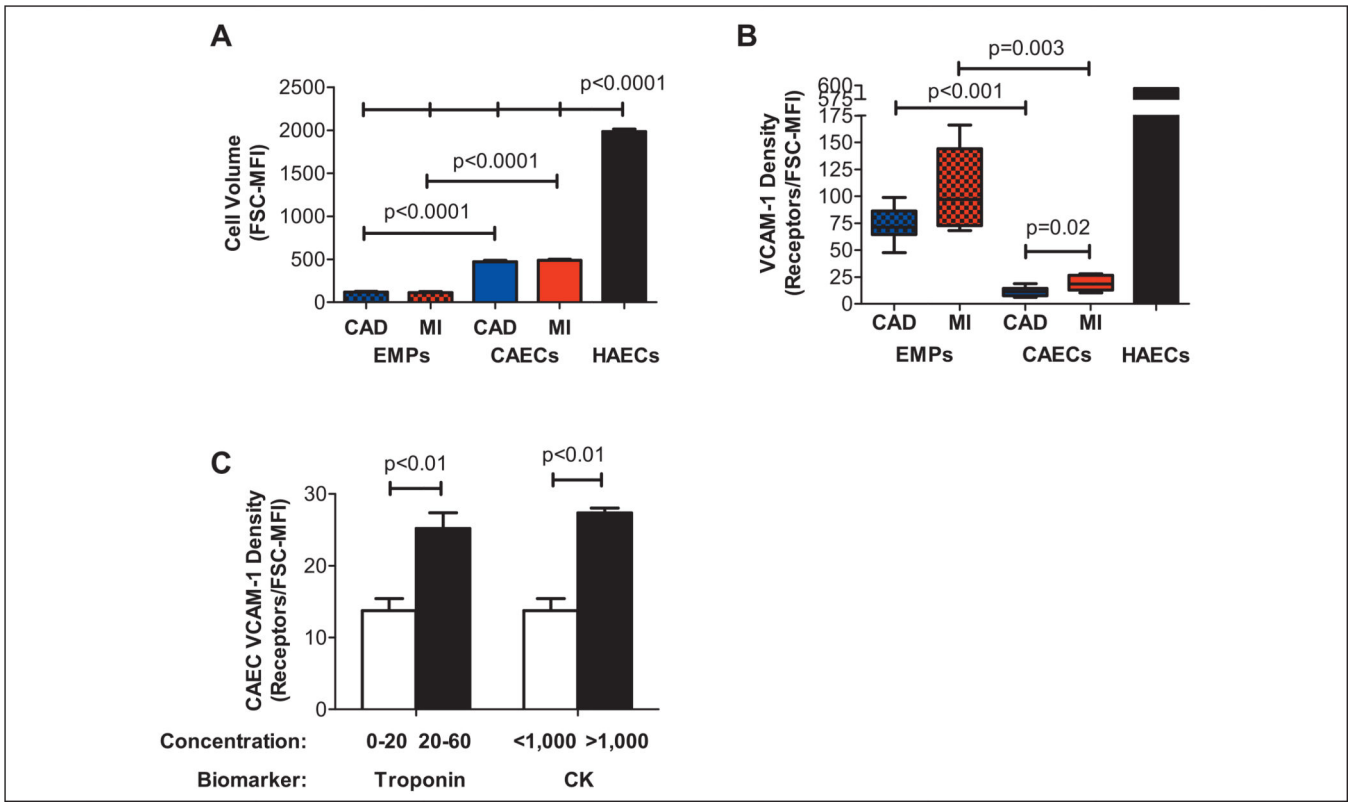

Figure 5. Cell volume, VCAM-1 density, and association of VCAM-1 density with markers of myocardial injury

A) Cell volumes estimated from forward light scatter were determined for stable CAD (117 ± 11 channels, n=13) and MI (111 ± 14 channels, n=5) EMPs, stable CAD (472 ± 17 channels, n=19) and MI (489 ± 13 channels, n=7) CAECs, and HAECs (1,985 ± 29 channels). EMPs were significantly smaller than CAECs ($p< 0.0001$ for stable CAD CAECs and stable CAD EMPs; $p< 0.0001$ for MI CAECs and MI EMPs; $p< 0.0001$ for stable CAD and MI EMPs and CAECs compared to HAECs; all analysis via unpaired t-test). B) VCAM-1 density (Receptors / FSC-MFI) for TNFα-stimulated (0.3 ng/ml) HAECs, stable CAD and MI CAECs, and stable CAD and MI EMPs. VCAM-1 density was computed from the product of the ratios of VCAM-1 to CD146 and CD146 to FSC as described in *Materials and methods*. VCAM-1+ CAECs expressed approximately 2–3 % of the VCAM-1 density of stimulated HAECs (stable CAD: 1.9 ± 0.2 %, n=13; MI: 3.1 ± 0.4 %, n=7; $p=0.02$ for stable CAD vs MI VCAM-1 densities, Mann-Whitney test). Stable CAD EMPs expressed significantly higher VCAM-1 densities relative to CAECs (stable CAD: 12.5 ± 2.5 %, n=13; MI: 17.9 ± 3 %, n=5; $p< 0.001$ for stable CAD EMPs vs stable CAD CAECs; $p=0.003$ for MI EMPs vs MI CAECs; $p=0.09$ for stable CAD EMPs vs MI EMPs; all analysis via Mann-Whitney test). Box and whisker plot shows 5th and 95th percentile whiskers, 25th and 75th percentile boxes, and median values. C) Relationship of CAEC expression of VCAM-1 with markers of myocardial injury is shown. VCAM-1 receptor density (VCAM-1 receptors / FSC-MFI) for VCAM-1^{+} CAECs from the MI subset was positively correlated with larger infarct size as determined by peak troponin ($p< 0.01$) and peak creatine kinase levels ($p<$

0.01). This data indicates the potential of activated CAECs as a novel marker for infarct size and cardiovascular risk.

Table 1

Clinical characteristics of patients. Stable CAD and MI patient population data. Mean ± standard deviation and p value statistics (unpaired Student t-test or Fisher's exact test) for each clinical characteristic. Significant differences between CAD and MI patients were present for age (p=0.01), white blood cell count (p< 0.001), troponin peak (p< 0.001), creatine kinase peak (p=0.001), and CKMB peak (p< 0.001) (displayed in bold).

Clinical characteristic	**CAD (N=47)**	**MI (N =25)**	**P-value**
Age (Years)	68.5 ± 11.8	61.2 ± 12.0	0.01
Male	37 (79 %)	18 (72 %)	0.57
Hypertension	40 (85 %)	18 (72 %)	0.22
Diabetes	17 (36 %)	8 (32 %)	0.80
Current Smoker	9 (19 %)	5 (20 %)	1.00
Past Smoker	23 (49 %)	13 (52 %)	1.00
Dyslipidaemia	43 (91 %)	22 (88 %)	0.69
Prior MI	24 (51 %)	7 (28 %)	0.08
LDL (mg/dl)	90.7 ± 26.14	97.5 ± 37.5	0.45
HDL (mg/dl)	42.2 ± 12.4	46.1 ± 22.1	0.40
TG (mg/dl)	146.5 ± 85.3	138.5 ± 93.0	0.74
Total Cholesterol (mg/dl)	156.6 ± 30.7	171.1 ± 39.6	0.13
Creatinine (ng/ml)	1.3 ± 0.9	1.3 ± 1.1	0.94
WBC Count (x 1e6/ml)	6.6 ± 1.5	9.1 ± 3.8	< 0.001
Platelet Count (x 1e6/ml)	212.6 ± 69.29	221.7 ± 80.8	0.62
Circumflex	18 (38 %)	10 (40 %)	1.00
LAD	16 (34 %)	7 (28 %)	0.79
RCA	13 (28 %)	7 (28 %)	1.00
Troponin Peak (ng/ml)	0.01 ± 0.02	17.4 ± 21.5	< 0.001
CK Peak (U/l)	44.3 ± 83.2	965.4 ± 1,653	< 0.001
CKMB Peak (μg/l)	2.9 ± 10.4	75.6 ± 109.8	< 0.001
BNP (pg/ml)	583.0 ± 769.8	359.6 ± 460.0	0.40
Target lesion length	18 ± 6	19 ± 9	0.55
Extent of CAD			0.53
One-Vessel	16 (34)	10 (40)	
Two-Vessel	15 (32)	6 (24)	
Three-Vessel	16 (34)	9 (36)	
SYNTAX score	14 ± 14	17 ± 14	0.48

Table 2

Comparison of MNC isolation and blood lysis methods for CAEC identification

Mean ± SEM values for relative HAEC cell counts (per 1,000 MNCs) for MNC isolation and blood lysis methods. MNC and lysed whole blood samples were titrated at a target HAEC to MNC concentration of 1 HAEC per 1,000 MNCs. The concentration was determined by hemocytometer for HAEC counts and by averaging three complete blood cell counts for MNC numbers (n=3; p=0.22, paired student t test, comparing the mean sampled HAECs per 1,000 MNCs for the two methods).

Method	HAECs per 1,000 MNCs[#]
MNC Isolation	1.19 ± 0.09
Blood Lysis	1.77 ± 0.39

[#]Theoretical mean: 1 HAECs per 1,000 MNCs.

Table 3

Comparison of endothelial cell counts from peripheral and coronary artery blood sources

Mean ± SEM values for relative (stable CAD n=19, MI n=8) and absolute (stable CAD n=13, MI n=8) cell counts for peripheral blood CECs and coronary blood-derived CAECs. Cell yield on balloon- derived CAECs was low, with a mean of 21.1 CAEC per balloon (stable CAD n=7, MI n=2). Significant p values are displayed in bold.

Blood Source		% of MNCs	vs. CECs	Cells / ml	vs. CECs
Peripheral (CECs)		0.03 ± 0.01		626.3 ± 235.7	
Coronary Artery (CAECs)	Stable CAD	0.09 ± 0.02	0.055	2,283 ± 688	0.07
	MI	0.12 ± 0.03	0.04	2,854 ± 1,093	0.05